Available online at www.sciencedirect.com
ScienceDirect
Energy Reports 8 (2022) 1011–1019
www.elsevier.com/locate/egyr

The 5th International Conference on Electrical Engineering and Green Energy, CEEGE 2022, 8–11 June, Berlin, Germany

Comparative analysis of dual active bridge *dc–dc* converter employing Si, SiC and GaN MOSFETs for G2V and V2G operation

Shishir S. Trivedi, Amit V. Sant*

Department of Electrical Engineering, School of Technology, Pandit Deendayal Energy University, Gandhinagar, India

Received 22 July 2022; accepted 6 August 2022
Available online 26 August 2022

Abstract

Electric vehicles (EVs) are ideally suited for carbon footprint reduction and energy-efficient transportation. EV battery chargers comprise of cascade connection of *ac–dc* and *dc–dc* converters. With the bidirectional *dc–dc* converters, EV chargers can implement grid-to-vehicle (G2V) and vehicle-to-grid (V2G) functionality. Dual active bridge (DAB) converter is a bidirectional *dc–dc* converter that can support G2V and V2G operation. DAB converters are operated at high switching frequencies (f_{sw}) leading to higher switching loss. This issue can be addressed by employing SiC and GaN-MOSFETs, which work with lesser switching losses and can operate at much higher f_{sw}. This paper presents a detailed comparative analysis of DAB converter employing Si, SiC and GaN MOSFETs for G2V and V2G operation. The EV charging system with a DAB converter employing V2G and G2V operation is modeled in PSIM software. Single phase shift (SPS) modulation technique is employed for DAB converter. The system operation is analyzed for V2G and G2V operation with the f_{sw} of 20 kHz, 50 kHz, 100 kHz and 200 kHz. The performance comparison reveals that DAB converter with GaN-MOSFETs has the highest operating efficiency. To validate the DAB operation with SPS modulation, experimental studies have been carried out with SPS modulation being implemented on TMS320F28335 DSP using SimCoder Module of PSIM. A step-by-step procedure to implement the modulation technique with SimCoder is also provided.

Peer-review under responsibility of the scientific committee of the 5th International Conference on Electrical Engineering and Green Energy, CEEGE, 2022.

Keywords: Battery chargers; Dual active bridge *dc–dc* converters; Electric vehicles; Single phase shift modulation; Wide bandgap switches

1. Introduction

Electric vehicles (EVs) are gaining prominence due to their merits of zero emissions, energy-efficient operation, and freedom from fossil fuels [1], which can lead to a significant reduction in carbon emissions from the transportation sector and can positively impact the climate change. In EVs, battery supplies the necessary power to propel the vehicle and needs frequent charging. The battery is charged through battery chargers, which usually

* Corresponding author.
E-mail address: amit.sant@sot.pdpu.ac.in (A.V. Sant).

https://doi.org/10.1016/j.egyr.2022.08.100

Peer-review under responsibility of the scientific committee of the 5th International Conference on Electrical Engineering and Green Energy, CEEGE, 2022.

comprise of cascade connection of *ac–dc* and *dc–dc* converters. With a unidirectional *dc–dc* converter, the EV batteries can get charged by drawing power from the grid. This operation is termed as grid to vehicle (G2V). However, in modern power systems, EVs can play an active role not only as a programmable load, but also as a distributed energy resource. With vehicle to grid (V2G) operation, EV batteries can supply power to the grid, especially during peak load conditions, and local loads, in case of microgrids. With V2G operation, EV chargers need to facilitate bidirectional power flow, which necessitates the use of a bidirectional *dc–dc* converter.

Among the different bidirectional *dc–dc* converters, dual active bridge (DAB) converter is ideally suited for EV chargers owing to its advantages of galvanic isolation, high energy density, higher power ratings, and energy efficiency operation [2,3]. Due to these advantages, the DAB converter is ideally suited for electric prolusion and battery charging systems. Adireddy et al. have illustrated the detailed circuit analysis of DAB converter and presented relevant simulation studies [3]. This converter consists of two H-bridge converters, HB-1 & HB-2, connected at the primary and secondary of a high frequency transformer (HFT). The direction of the flow of power depends on phase shift between the gate pulse applied to the HB-1 and HB-2. For the flow of power from primary to the secondary, the gate signals to the HB-1 leads that of the HB-2. Alternately, if the gate signals to the HB-1 lags the gate signals to the HB-2, the direction of power flow is reversed. Moreover, by controlling the exact value of phase-shift, the output voltage can also be controlled. Refs. [4–8] have reported DAB converter for different EV applications. Li et al. and Xue et al., and Assadi et al. have reported the use of DAB converters for off-board and on-board charging, respectively [4,6]. Also, DAB converter has been employed for charging a plug-in hybrid EV [5]. SiC and GaN switches based DAB converter is explored in [7]. Ref. [8] investigated EV charging with single phase shift (SPS) modulation strategy modulated DAB converter. SPS modulation strategy is the generally preferred strategy for DAB converters due the ease of its implementation [9,10].

The DAB converter operates at high switching frequencies (f_{sw}), which results in higher switching losses and reduced converter efficiency. Lower f_{sw} would result in an increased size of HFT. Wide bandgap switches can overcome this and allows the switches to operate at higher f_{sw} with lower switching losses. As compared to Si switches, the wide bandgap switches based on SiC and GaN can effectively operate at higher f_{sw}, voltage ratings and temperatures with lower switching losses. With the prime focus on energy conservation, the use of battery chargers with wide bandgap switches would be a norm in the near future. A detailed comparison of DAB converters using Si, SiC, and GaN MOSFETs for G2V and V2G operation is presented in this paper. PSIM software is used to model the V2G and G2V operation of an EV charger system comprising of a DAB converter. The DAB converter is implemented with single phase shift (SPS) modulation technique. With the help of the respective datasheets, the practical characteristics of the Si, SiC, and GaN MOSFETs are incorporated into the simulation model through Thermal Module. The operation of the system is investigated for V2G and G2V operation at f_{sw} = 20, 50, 100, and 200 kHz. The comparative analysis reveals that the DAB converter with GaN-MOSFETs outperforms the other two switches in terms of switching and conduction losses at selected frequencies. An experimental prototype of DAB converter is developed with TMS320F28335 DSP based implementation of SPS control scheme. SimCoder Module of PSIM is utilized for developing the necessary code. The step-by-step procedure for the SimCoder based implementation is also discussed.

2. Operation and analysis of dual active bridge *dc–dc* converter

Fig. 1 Shows the power structure and DSP based implementation modulation technique for a DAB converter. The power circuit consists of two H-bridge converters, HB-1 & HB-2, connected at the primary and secondary of a HFT. A high frequency inductor L_{lk} is used to interface HB-1 with the primary winding. The primary to secondary turns ratio of HFT is N:1. HB-1 consists of four power MOSFETs, S_1–S_4, and HB-2 comprises of four power MOSFETs, S_5–S_8. In HB-1 and HB-2, the pair of diagonal switches are turned ON with the other pair being turned OFF. All the MOSFETs operate at 50% duty cycle and the MOSFETs in the same leg are not turned ON at the same time to prevent short-circuiting of the *dc* source. A *dc* source V_{in} is connected at the input of HB-1 and a battery is connected at the output of HB-2. The output voltage of the HB-2 is V_o. HB-1 operates as an inverter to provide high frequency square wave at the primary winding. Based on the turns ratio, the stepped up or stepped down *ac* voltage appears at the secondary winding. HB-2 acts as a rectifier and facilitates the availability of regulated *dc* supply at the battery terminals. A filter capacitor, C_o, is connected at the output to filter out the ripple in V_o. This operation, wherein the power flows from V_{in} to the battery is possible only when the gate pulses applied to HB-1 leads to those applied to HB-2. If the gate pulse of HB-2 are leading the gate pulse of HB-1, then the power would

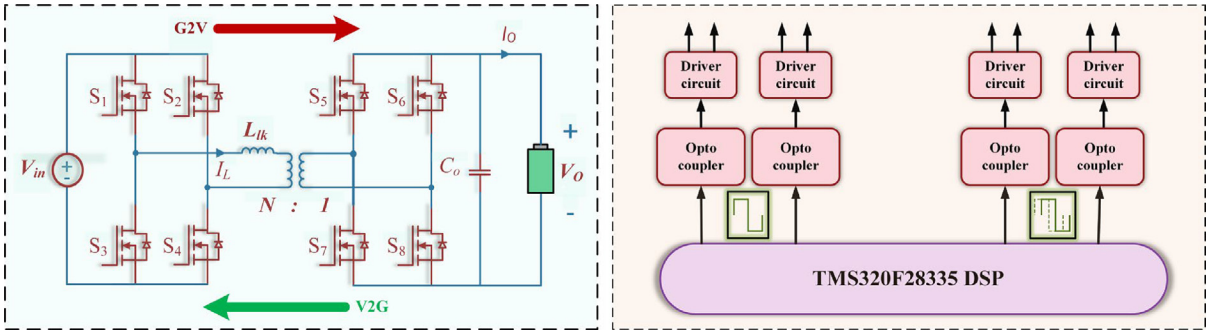

Fig. 1. Power and control circuit configuration of dual active bridge dc–dc converter.

flow from the battery to V_{in}. This technique involving the introduction of phase shift between the gate signals of HB-1 and HB-2 to facilitate the flow of power from the leading bridge to the lagging bridge is referred to as the single phase shift (SPS) modulation. The control circuitry of the DAB converter consists of a DSP, an optocoupler and a driver circuit. The DSP is used to generate the phase shifted gating signals for HB-1 and HB-2. Optocoupler is used to provide isolation between the DSP and the power circuitry. Lastly, the driver circuit provides the required biasing, after which the gating signals are supplied to the corresponding power MOSFETs.

The operation of DAB converter can be analyzed through the waveforms and switching table provided in Fig. 2 and Table 1, respectively. The inductor current for different operating states depends on the difference in the primary and secondary voltages of HFT, denoted as V_P and V_S. The operational and mathematical analysis of inductor current is performed for six operating states, assuming that the DAB converter operates in buck mode in forward conduction and boost mode in reverse conduction mode, i.e., $V_P > V_S$. For each operating state, based on the conducting switches/diodes, the equations of inductor current for the corresponding intervals are derived as summarized in Table 1.

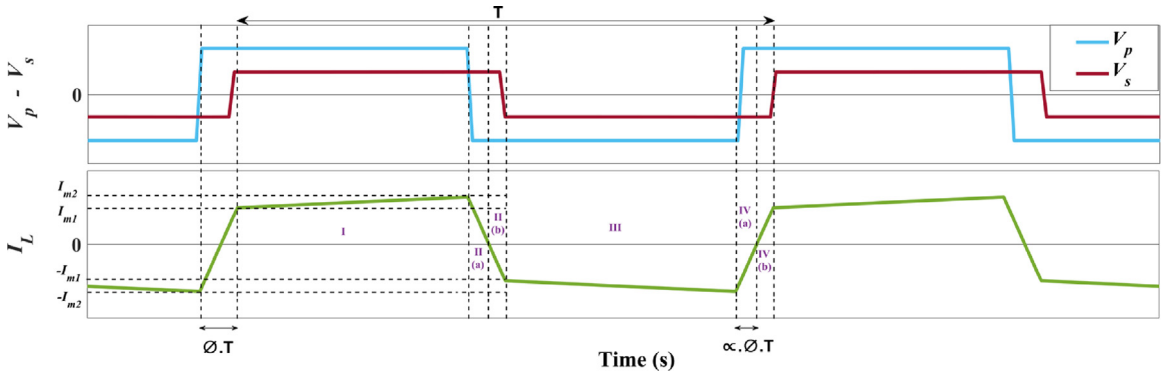

Fig. 2. Operational analysis of dual active bridge *dc–dc* converter.

3. Implementation of single phase shift modulation using SimCoder module in PSIM

The SPS modulation technique is widely used in DAB converters for power transfer in either direction due to its simplicity [9,10]. The direction and amount of the power flow depend on the phase shift between the gating signals of HB-1 and HB-2. SPS modulation technique can be implemented with TMS320F28335 DSP using SimCoder module available in PSIM software. PSIM has a hardware target for TMS320F28335 DSP and SimCoder module for automatic code generation. SimCoder based code generation of control system can be easily implemented, which is significantly helpful for testing and rapid prototyping. The step-by-step procedure for the implementation of SPS modulation for the DAB converter using the SimCoder module is provided in Table 2.

Table 1. Mathematical analysis of different operating states of the dual active bridge *dc–dc* converter.

Duration	Conducting switches	V_L	I_L
I	S_1, S_4, D_5, D_8	$V_P - V_S$	$I_{m1} + (V_{in} - V_o) . (T - T.\varnothing) / L$
II-(a)	S_2, S_3, D_5, D_8	$-V_P - V_S$	$I_{m2} + (-V_{in} - V_o) . (\propto .T.\varnothing) / L$
II-(b)	S_2, S_3, S_5, S_8	$-V_P - V_S$	$(-V_{in} - V_o) . ((1- \propto) .T.\varnothing) / L$
III	S_2, S_3, D_6, D_7	$-V_P + V_S$	$-I_{m1} + (-V_{in} + V_o) . (T - T.\varnothing) / L$
IV-(a)	S_1, S_4, D_6, D_7	$V_P + V_S$	$-I_{m2} + (V_{in} - V_o) . (\propto .T.\varnothing) / L$
IV-(b)	S_1, S_4, S_6, S_7	$V_P + V_S$	$(V_{in} + V_o) . ((1- \propto) .T.\varnothing) / L$

Table 2. Step-by-step procedure for the SimCoder based implementation of SPS modulation for dual active bridge *dc–dc* converter.

Steps	Description
1.	*Generation of gate pulses for HB-1 and HB-2* – 1-Phase PWM and 1-Phase PWM phase shift blocks are used to generate gate pulses for HB-1 and HB-2, respectively. The parameters in these blocks, such as switching frequency, duty cycle, and dead time are correspondingly configured to values 10 kHz, 50% and 4µs based on the design and requisite operation of the DAB converter. – The output mode of the PWM blocks is selected as 'PWM A & B'. The 'A' output terminal provides the desired PWM output, and the 'B' output terminal provides the PWM signal that is conjugated of A. – Duty cycle is an input parameter for the 1-Phase PWM block, which is compared with the carrier signal of mentioned switching frequency so as to generate the necessary gating signals for HB-1. A sawtooth carrier wave with the peak-to-peak value of 1 is selected. The duty cycle input is realized using a *dc* source connected to the *'in'* terminal of the PWM blocks. The *dc* source's magnitude signifies the duty cycle to be implemented, which is 0.5 for the DAB converter. – 1-Phase PWM phase shift block has two inputs; duty cycle and phase shift. For applying a phase shift to the PWM signals of the HB-2, a constant block is connected at the '*phase*' terminal of the 1-Phase PWM phase shift block. The value of the constant block denotes the phase shift in degrees. This will produce gate signals phase shifted with respect to the PWM block employed for the HB-1. – A different PWM source number is assigned in 1-Phase PWM phase shift block to have distinct output at distinct GPIO pins i.e., for PWM 1; GPIO pins 0 and 1 are used, for PWM 2; GPIO pins 2 and 3 are used and so on.
2.	*Marking the hardware GPIO pins for extraction of generated gate pulses* – The DAB converter employs a four pins to generate PWM signals, i.e., GPIO0 for switches S_1 and S_4, GPIO1 for switches S_2 and S_3, GPIO2 for switches S_5 and S_8, and GPIO3 for switches S_6 and S_7. – The GPIO pins used as per the PWM source assigned in the PWM blocks are marked and locked in the hardware configuration block.
3.	*Setting the DSP's clock frequency* – DSP clock is set at its maximum limit, i.e., 150 MHz. The external clock is the frequency of the DSP board. The DSP speed must be set as an integer multiple of the external clock.
4.	*Assigning the hardware target for dumping the generated code* – The hardware target in the simulation control block is set to the target F28335 DSP. RAM debug is selected to dump the generated C code in the RAM.
5.	*Generation and Flashing of the C code on DSP board* – The code is generated automatically based on the simulation model of the control logic implemented on the PSIM simulation software consisting of SimCoder block set – The generated C code is flashed into the DSP using code composer studio software which is used for communicating information between a pc and DSP. Hence, the implementation of SPS modulation for the DAB converter is achieved with the DSP generating the desired gating signals for HB-1 and HB-2.

4. Thermal module-based efficiency evaluation of DAB converter implemented with wide bandgap switches

Wide bandgap semiconductors, i.e., SiC and GaN based power semiconductor switches, are widely adopted due to their ability to operate at a higher f_{sw}, higher voltage ratings, higher temperatures, and lesser switching losses due to lower on-state resistance compared to Si power semiconductor switches. As the DAB converter operates at high f_{sw}, wide bandgap switches play an essential role in implementing an efficient DAB converter based compact fast EV battery charger. To design an efficient bidirectional EV charger, the charger with the best efficiency for the power flowing in either direction is preferred.

PSIM has a Thermal Module that simulates the practical characteristics of a power semiconductor switch based on the device datasheet without slowing down the simulation speed. It is employed to estimate a power semiconductor

switch's conduction and switching loss and to study its performance during different operating conditions. Three different power MOSFETs with similar ratings are configured into PSIM with the help of the Thermal Module: 650 V, 60 A GaN MOSFET GS66516, 650 V, 58 A SiC MOSFET IMW65R030M1H, and 650 V, 58 A Si MOSFET NVHL050N65S3HF. At 20 and 50 kHz, the operation of DAB converter with all the three MOSFETs is analyzed. For 100 and 200 kHz, DAB converter operation with SiC and GaN MOSFETs is analyzed. In G2V mode, the DAB converter is simulated for operating in buck mode for charging BWP-FE51100-ATI-PF Li-ion battery pack that supports a maximum 58.4 V and 50 A of charging voltage and current, respectively. The input voltage of 325 V and phase shift of 25° is implemented. Similarly, for V2G mode, the designed DAB converter is simulated in boost mode to provide a constant output *dc*-link voltage of 325 V.

Switching and conduction losses for individual MOSFETs are evaluated for G2V and V2G operating modes. Tables 3 and 4 summarize the results of Si, SiC, and GaN based DAB converter operating in G2V and V2G modes, respectively. The results are based on $f_{sw} = 50$ kHz. The $P_{s1} - P_{s8}$ and $P_{cd1} - P_{cd8}$ denote the switching losses and conduction losses occurring in the switches $S_1 - S_8$, respectively. The diagonal pair of switches exhibit similar switching and conduction losses in HB-1 and HB-2 due to their simultaneous turn ON and OFF. For G2V mode, the switching losses in HB-1 and HB-2 with Si MOSFETs is higher due to the poor switching characteristics with the increase in f_{sw}. The SiC MOSFETs exhibit a significant conduction loss in HB-2 due to greater I^2R losses in their body diodes. The GaN MOSFETs show an efficient operation in HB-1 and HB-2 with minimum conduction and switching losses, thereby validating its practical switching characteristics. Similarly, Si, SiC, and GaN based DAB converters are simulated in V2G mode operating at 50 kHz. For V2G mode, the magnitude of current drawn by the inductor increases, accounting for greater conduction losses in HB-2, as evident from the results presented in Table 4. The GaN based DAB converter has the least switching and conduction losses, whereas the Si MOSFET exhibits almost double the losses compared to GaN MOSFETs. Thus, it is concluded that the GaN MOSFETs retain their efficient operation in both V2G and G2V modes. SiC MOSFETs show satisfactory operation with minimal change in losses during the switching of the modes. Lastly, the Si MOSFET exhibits the greatest power losses in both cases, with 36.97% and 80.96% more losses than the GaN MOSFETs in G2V and V2G operation modes.

Table 3. Switching and conduction losses for individual MOSFETs for the DAB operating in G2V mode at 50 kHz.

Power MOSFET employed	Bridge	Switching losses (W)				Conduction losses (W)				Total losses (W)
		P_{S1}/P_{S5}	P_{S2}/P_{S6}	P_{S3}/P_{S7}	P_{S4}/P_{S8}	P_{cd1}/P_{cd5}	P_{cd2}/P_{cd6}	P_{cd3}/P_{cd7}	P_{cd4}/P_{cd8}	
Si	HB-1 (S_1-S_4)	3.1973	3.1994	3.1994	3.1973	0.7797	0.7754	0.7754	0.7797	71.2162
	HB-2 (S_5-S_8)	0.3737	0.3757	0.3757	0.3737	13.466	13.440	13.440	13.466	
SiC	HB-1 (S_1-S_4)	0.7927	0.7942	0.7942	0.7927	0.5725	0.5707	0.5707	0.5457	63.8476
	HB-2 (S_5-S_8)	0.2438	0.2445	0.2445	0.2438	14.335	14.247	14.491	14.335	
GaN	HB-1 (S_1-S_4)	0.5071	0.5070	0.5070	0.5071	0.4784	0.4767	0.4767	0.4784	51.9916
	HB-2 (S_5-S_8)	0.0740	0.0741	0.0741	0.0740	11.982	11.896	11.896	11.982	

Table 4. Switching and conduction losses for individual MOSFETs for the DAB operating in V2G mode at 50 kHz.

Power MOSFET employed	Bridge	Switching losses (W)				Conduction losses (W)				Total losses (W)
		P_{S1}/P_{S5}	P_{S2}/P_{S6}	P_{S3}/P_{S7}	P_{S4}/P_{S8}	P_{cd1}/P_{cd5}	P_{cd2}/P_{cd6}	P_{cd3}/P_{cd7}	P_{cd4}/P_{cd8}	
Si	HB-1 (S_1-S_4)	3.5597	3.5599	3.5599	3.5597	0.7251	0.7228	0.7228	0.7251	90.8026
	HB-2 (S_5-S_8)	0.3646	0.3633	0.3633	0.3646	18.110	18.001	18.001	18.110	
SiC	HB-1 (S_1-S_4)	0.9276	0.9277	0.9277	0.9276	0.5457	0.5427	0.5427	0.5457	60.8079
	HB-2 (S_5-S_8)	0.1230	0.1252	0.1252	0.1230	13.617	13.593	13.593	13.617	
GaN	HB-1 (S_1-S_4)	0.5571	0.5571	0.5571	0.5571	0.4606	0.4577	0.4577	0.4606	50.1761
	HB-2 (S_5-S_8)	0.0478	0.0478	0.0478	0.0478	11.490	11.468	11.468	11.490	

A comparative analysis is presented in Table 5 to assess the efficiency of the DAB converters in PSIM simulation platform. For the comparative analysis, three DAB converters are modeled in PSIM, each comprising of (a) Si MOSFETs, (b) SiC MOSFETs, and (c) GaN MOSFETs. The magnetic components are separately designed for

Table 5. DAB converter implemented with different MOSFETs under different operating conditions and modes.

Type of power MOSFET employed	Frequency (kHz)	Grid-to-Vehicle mode			Vehicle-to-Grid mode		
		HB-1 losses (W)	HB-2 losses (W)	Efficiency (%)	HB-1 losses (W)	HB-2 losses (W)	Efficiency (%)
Si	20	6.584	55.772	96.228	6.395	79.575	95.551
SiC	20	2.910	58.393	96.576	2.995	58.197	96.316
GaN	20	2.247	48.643	97.161	2.277	48.575	97.080
Si	50	15.904	55.313	96.228	17.329	73.289	94.724
SiC	50	5.460	58.143	96.634	5.925	54.404	96.509
GaN	50	5.644	48.389	97.137	4.083	45.682	97.134
SiC	100	6.845	57.271	96.395	6.997	54.402	96.268
GaN	100	13.303	47.794	96.578	4.745	47.325	96.838
SiC	200	15.969	53.510	95.981	15.756	51.862	95.718
GaN	200	11.058	43.890	96.795	8.421	37.239	97.006

the DAB converters operating at four different f_{sw} i.e. 20, 50, 100, and 200 kHz. The performance of the DAB converters are examined in G2V and V2G modes under different operating frequencies based on the optimal f_{sw} range of the practically modeled MOSFETs. At f_{sw} of 20 kHz, GaN based DAB converter exhibits highest efficiency i.e., 97.161% and 97.080% in G2V and V2G modes, respectively. Si and SiC have a significantly greater conduction losses in the HB-2 for V2G mode, thereby decreasing its overall efficiency. For DAB converters operating at f_{sw} of 50 kHz, the results verify the efficient operation of GaN based DAB converters over Si and SiC with the least amount of power losses. The efficiency of GaN based DAB converter for G2V and V2G mode of operation is obtained as 97.137% and 97.134%, respectively. For f_{sw} of 100 kHz the comparative analysis is carried out for SiC and GaN MOSFETs as the f_{sw} lies beyond the optimal range of operation for Si MOSFETs. The operation of GaN based DAB converter shows an efficiency of 96.578% and 96.838% in G2V and V2G modes. SiC exhibits marginally greater switching and conduction losses compared to GaN in both the modes. Lastly, for f_{sw} of 200 kHz, the GaN based DAB converter potrays the best efficiency, i.e., 96.795% and 97.006% in G2V & V2G modes respectively, compared to SiC based DAB converter. The Si-based DAB converter has the worst efficiency in both the modes of operation due to a greater amount of switching and conduction losses in the HB-2. The SiC based DAB converters show efficient operation in both modes under different f_{sw} compared to Si switches. In all the cases, the GaN based DAB converter exhibits the most efficient operation with minimal difference in efficiency in the event of switching the operation modes. Moreover, due to the efficient operation of wide bandgap switches at a higher f_{sw}, the DAB converter becomes more compact as the size of the magnetic components greatly reduces with the increase in operating frequency. Also, employing wide bandgap switches allows for a better thermal management system for an EV charger.

5. Simulation & experimental results

The designed DAB converter is simulated in PSIM simulation software with SPS modulation employing a phase-shift of 25° and $f_{sw} = 10$ kHz. Fig. 3 shows the simulated performance of the DAB, where $G_1 - G_8$ are the gate pulse for $S_1 - S_8$, respectively. Phase shift is apparent between the diagonal switch pairs of HB-1 and HB-2 and the across primary and secondary voltages. A steady-state *dc* output voltage of 24 V and a standard inductor current waveform with a peak-to-peak value of 2 A is observed.

Experimental prototype model of the DAB converter is shown in Fig. 4. The experimental model implements SPS modulation technique. The DAB converter is designed for a 50 W power rating feeding a regulated *dc* output of 24 V and 2 A to a resistive load at $f_{sw} = 10$ kHz. The input *dc* voltage is 50 V. HFT utilizes PQ 26/25 ferrite core rated at 50 Watts with 53 and 27 turns for primary and secondary winding, respectively. The high frequency inductor utilizes a toroid core rated at 10 A, 300 μH. The code for the generation of gate pulses for both the H-bridge converters is implemented with a TMS320F28335 DSP. The model for DSP based implementation is developed in PSIM using SimCoder module. Further, with the hardware target and code generation feature available in PSIM, the code is generated in C language. This code is flashed into TMS320F28335 DSP using code composer studio software. The gate signals generated from the DSP are applied to the corresponding H-bridge MOSFETs through

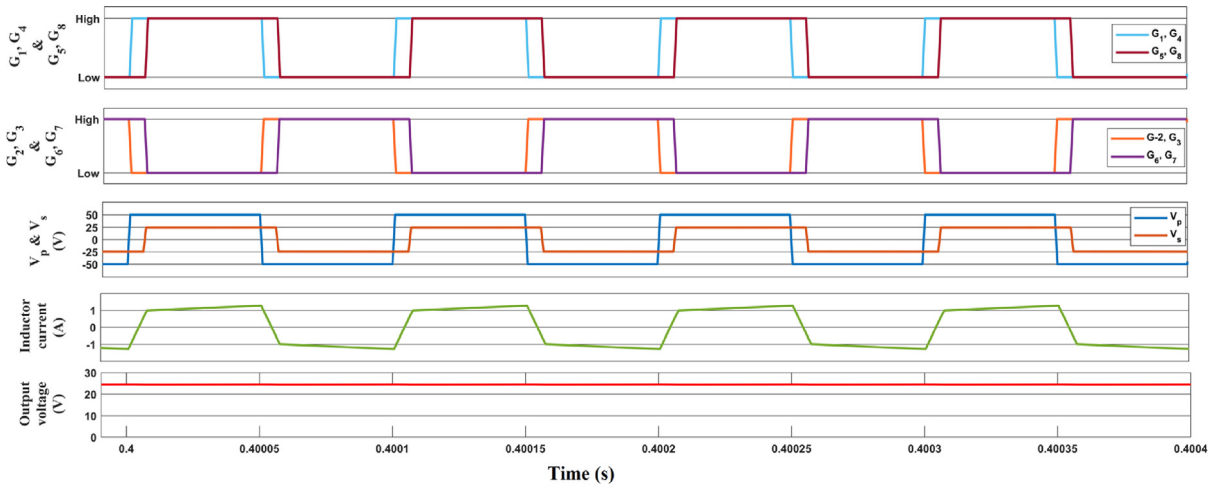

Fig. 3. Performance analysis of DAB converter with SPS control having phase-shift of 25°.

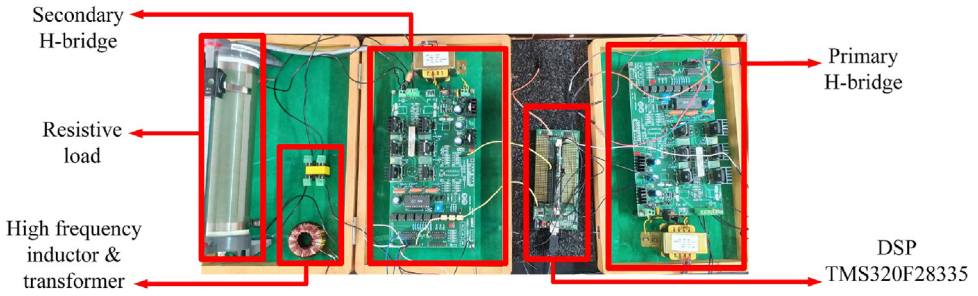

Fig. 4. DAB converter experimental model.

optocouplers and driver circuits. The experimental results examining the performance of DAB converter are shown in Fig. 5. The gating signal generated through the SimCoder method depicts a phase shift of 25° between HB-1 and HB-2 with a dead time of 4μs. The phase shifted primary and secondary voltages are illustrated by Fig. 5 (b). Distorted waveform in the primary voltage is observed due to the effect of the dead time, however; the average value of the voltage still remains zero. The primary and secondary have a peak-to-peak voltage of 100 V and 50 V, respectively. This is as per the turns ratio of 53:27 for the designed HFT. From Fig. 5 (c) it is clear that the output *dc* voltage is regulated 20 V. The peak-to-peak inductor current of 1 A at 25°. The output power is equal to the input minus the switching and conduction losses occurring in HB-1 and HB-2. Hence, the output power is less than the

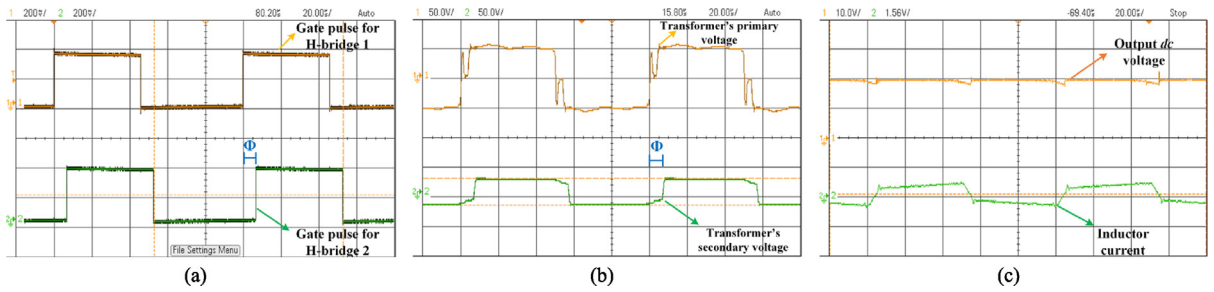

Fig. 5. DAB converter experimental studies: (a) gate pulses for HB-1 & HB-2, (b) HFT's primary & secondary voltage, (c) output *dc* voltage & inductor current.

theoretical value. The waveforms demonstrated through experimental results match the waveforms obtained through theoretical analysis and simulation studies. Therefore, it can be said that the DAB converter experimental model yields the expected output results as per the designed and simulated parameters. With the SimCoder module of PSIM rapid prototyping is possible with freedom to implement the control algorithm through the given block sets.

6. Conclusion

DAB converter is ideally used for EV charging application due to its ability to facilitate bidirectional power flow. As the DAB converter operates at high f_{sw}, switching losses are predominant in both the half-bridges. To implement an efficient EV charger, the traditionally employed Si switches are replaced with SiC and GaN switches to examine the efficiency of the DAB converter in G2V and V2G modes. The DAB based charging system is simulated by configuring the SiC and GaN switches according to their practical switch characteristics in PSIM software through the Thermal Module feature. This paper presents a detailed comparison of Si, SiC, and GaN based DAB converters under different f_{sw} and conduction modes. Si based DAB converter exhibits greater conduction and switching losses among the three switches, especially in V2G mode. In all the cases, the simulation studies verify the efficient operation of wide bandgap switches, especially GaN based DAB converters which shows a minimal change of efficiency in G2V and V2G modes. Moreover, due to the ability of wide bandgap switches to operate at a higher f_{sw}, the DAB converter becomes more compact as the size of the magnetic components greatly reduces. Experimental prototype model of DAB converter is developed with TMS320F28335 DSP based implementation of SPS control scheme. This paper also provides a step-by-step procedure to implement the modulation technique with SimCoder feature in PSIM software. The experimental results show a regulated output dc voltage of 20 V and the peak-to-peak inductor current of 1 A at 25°. The DAB converter experimental model implemented through SimCoder, provides the expected output results as per the designed and simulated parameters.

CRediT authorship contribution statement

Shishir S. Trivedi: Investigation, Formal analysis, Validation, Writing – original draft. **Amit V. Sant:** Conceptualization, Investigation, Supervision, Writing – review & editing.

Declaration of competing interest

The authors declare that they have no known competing financial interests or personal relationships that could have appeared to influence the work reported in this paper.

Data availability

No data was used for the research described in the article.

Appendix A. Supplementary data

Supplementary material related to this article can be found online at https://doi.org/10.1016/j.egyr.2022.08.100.

References

[1] Sanguesa JA, Torres-sanz V, Garrido P, Martinez FJ, Marquez-barja JM. Smart cities a review on electric vehicles : Technologies and challenges. Smart Cities 2021;2021(4):372–404.
[2] Ullah N, Farooq Z, Zaman T, Sami I, Ibeas A, Techato K, Chowdhury MS, Muyeen SM. A computationally efficient robust voltage control for a single phase dual active bridge. Energy Rep 2020;6:3346–56.
[3] Adireddy R, Pratap KNGA, Himaja T, Murthy KVSR. Circuit analysis and modelling of dual active bridge bidirectional converter. Mater Today Proc 2021.
[4] Li J, Wang D, Wang W, Jiang J. Minimize current stress of dual-active-bridge DC-dc converters for electric vehicles based on Lagrange multipliers method. Energy Procedia 2017;105:2733–8.
[5] Xue L, Shen Z, Boroyevich D, Mattavelli P, Diaz D. Dual active bridge-based battery charger for plug-in hybrid electric vehicle with charging current containing low frequency ripple. IEEE Trans Power Electron 2015;30:7299–307.
[6] Assadi SA, Member S, Matsumoto H. Active saturation mitigation in high-density dual-active-bridge DC-DC converter for on-board EV charger applications. IEEE Trans Power Electron 2019;35:4376–87.
[7] Yan Y, Bai H, Foote A, Wang W. Securing full-power-range zero-voltage switching in both steady-state and transient operations for a dual-active-bridge-based bidirectional electric vehicle charger. IEEE Trans Power Electron 2020;35:7506–19.

[8] Mirtchev A, Tatakis E. Design methodology based on dual control of a resonant dual active bridge converter for electric vehicle battery charging. IEEE Trans Veh Technol 2022;71:2691–705.
[9] Chen X, Member S, Xu G, Han H, Liu D, Member S, Sun Y, Su M. Light-load efficiency enhancement of converter under SPS control. IEEE Trans Ind Electron 2020;68:12941–6.
[10] Wei S, Zhao Z, Li K, Yuan L, Wen W. Deadbeat current controller for bidirectional dual-active-bridge converter using an enhanced SPS modulation method transactions on power electronics. IEEE Trans Power Electron 2020;36:1274–9.